A Combined Pyro- and Hydrometallurgical Approach to Recycle Pyrolyzed Lithium-Ion Battery Black Mass Part 1: Production of Lithium Concentrates in an Electric Arc Furnace

Marcus Sommerfeld [1,*], Claudia Vonderstein [1], Christian Dertmann [1], Jakub Klimko [2], Dušan Oráč [2], Andrea Miškufová [2], Tomáš Havlík [2], Bernd Friedrich [1]

[1] IME Process Metallurgy and Metal Recycling, Institute of RWTH University; Intzestraße 3, 52056 Aachen, Germany; msommerfeld@ime-aachen.de (M.S.); cvonderstein@ime-aachen.de (C.V.); cdertmann@ime-aachen.de (C.D.); bfriedrich@ime-aachen.de (B.F.)

[2] IRT-Institute of Recycling Technologies; Letna 9, 042 00 Košice, Slovakia; jakub.klimko@tuke.sk (J.K.); dusan.orac@tuke.sk (D.O.); andrea.miskufova@tuke.sk (A.M.); tomas.havlik@tuke.sk (T.H.)

*Correspondence: msommerfeld@ime-aachen.de; Tel.: +492418095200

S1. Supplementary Information about the Slag

This chapter includes supplementary material about the slag phase obtained in this research.

Figure S1 shows macrographs of two slag samples. Even though the chemical composition is rather similar, they differ in visual appearance. Sample (a) was tapped after the trial and was cooled with a higher cooling rate compared to sample (b), which was solidified in the crucible after the trial.

(a)   (b)

Figure S1. Macrographs of slag: (a) generated in trial number 5, (b) generated in trial number 6.

Table S1 lists the information card number for the used minerals in the X-ray diffraction analysis from the Crystallography Open Database.

Table S1. Chemical Formula, mineral name and information card number.

Chemical Formula	Mineral	Information Card Number
$LiAlSiO_4$	Beta-Eucryptite	8104279
$LiAlO_2$	Gamma-Lithium Aluminium Oxide	1008166
Li_2SiO_3	Lithium Metasilicate	2310662
$LiAlSiO_4-SiO_2$	Beta-Eucryptite	9002380

Table S2 shows the complete chemical analysis of slag samples taken after the trial and during the holding time of the trials.

29

Table S2. Chemical composition of slag samples taken during the holding time and after solidification.

No.	Addition in g per 100 g black mass		Sampling Time during Holding	ICP-OES analysis in wt.%				Combustion in wt.%		XRF in wt.%											
	Quartz	CuO	t in min	Li	Cu	Co	Ni	C	S	SiO_2	TiO_2	Al_2O_3	Fe_2O_3	Mn_3O_4	MgO	CaO	Na_2O	K_2O	P_2O_5	ZrO_2	BaO
1	20 g	95 g	0	4.23	3.59	1.70	0.17	*	*	51.9	0.32	19.9	2.71	2.48	0.42	0.44	0.60	0.93	0.176	0.09	0.50
1	20 g	95 g	10	5.25	1.46	0.76	0.06	*	*	54.9	0.11	21.0	2.74	2.73	0.43	0.45	0.46	0.95	0.102	0.10	0.52
1	20 g	95 g	After trial	5.53	0.23	0.09	0.01	0.029	0.017	56.2	0.12	22.0	0.52	2.25	0.46	0.47	0.35	0.98	0.02	0.10	0.57
2	20 g	90 g	0	4.27	3.12	1.78	0.13	*	*	53.2	0.11	20.3	2.91	2.29	0.44	0.43	0.53	0.86	0.164	0.09	0.50
2	20 g	90 g	After trial	5.18	1.4	1.44	0.05	0.035	0.020	53.4	0.11	20.2	2.25	2.23	0.43	0.45	0.38	0.86	0.150	0.09	0.50
3	20 g	80 g	0	4.98	1.17	0.97	0.06	*	*	48.2	0.13	26.2	1.79	1.88	0.67	1.29	0.64	0.73	0.117	0.13	0.67
3	20 g	80 g	10	4.90	0.13	0.13	0.07	*	*	50.4	0.15	27.5	0.36	1.88	0.66	1.33	0.62	0.72	0.019	0.13	0.70
3	20 g	80 g	After trial	5.84	0.39	0.41	0.05	0.120	0.033	49.7	0.13	27.1	0.67	1.69	0.63	1.32	0.57	0.70	0.03	0.14	0.69
4	20 g	65 g	0	6.53	4.41	0.49	0.04	0.070	0.029	*	*	*	0.66#	0.85#	*	*	*	*	*	*	*
4	20 g	65 g	10	6.84	0.36	0.04	0.00	0.340	0.035	*	*	*	0.19#	0.94#	*	*	*	*	*	*	*
4	20 g	65 g	After trial	6.24	0.40	0.25	0.03	0.285	0.049	46.5	0.14	30.2	0.22	0.84	0.59	0.82	0.77	0.48	0.02	0.62	0.76
5	10 g	92.3 g	0	5.44	4.35	0.52	0.05	*	*	39.9	0.14	30.1	1.45	2.48	0.59	0.78	0.74	0.54	0.125	0.16	0.81
5	10 g	92.3 g	10	6.37	1.93	1.60	0.17	*	*	40.0	0.15	29.2	3.34	3.54	0.58	0.80	0.66	0.53	0.123	0.15	0.79
5	10 g	92.3 g	After trial	6.77	0.35	0.07	0.01	0.238	0.028	43.1	0.15	32.2	0.31	2.12	0.63	0.88	0.72	0.55	0.016	0.17	0.87
6	10 g	96.3 g	0	7.38	0.85	0.82	0.09	*	*	41.4	0.16	31.2	0.81	1.23	0.65	0.81	0.60	0.75	0.053	0.14	0.78
6	10 g	96.3 g	10	7.23	0.26	0.17	0.02	*	*	42.9	0.18	33.3	0.63	1.04	0.68	0.94	0.46	0.45	0.018	0.16	0.83
6	10 g	96.3 g	After trial	7.40	0.10	0.06	0.01	0.184	0.084	41.8	0.15	33.4	0.14	0.70	0.68	0.95	0.47	0.42	0.016	0.15	0.83

30 *not analyzed; #analyzed by ICP-OES compared to the other slag samples

31

32

33

34

35

36 Table S3 shows the standard deviation of the sample set presented in Table 4 in the main paper.

37 **Table S3**. Standard deviation of the chemical analyses presented in Table 4 in the main paper in wt.%.

Trial	Li	Cu	Co	Ni	C	SiO_2	Al_2O_3	Fe_2O_3	Mn_3O_4	BaO
1	0.010	0.006	0.007	0.001	0.003	1.038	0.424	0.023	0.028	0.009
2	0.043	0.041	0.044	0.000	0.002	0.486	0.204	0.021	0.010	0.001
3	0.010	0.010	0.002	0.005	0.001	0.060	0.131	0.021	0.008	0.004
4	0.006	0.001	0.011	0.001	0.007	0.098	0.084	0.018	0.016	0.002
5	0.006	0.010	0.002	0.000	0.005	0.075	0.021	0.024	0.000	0.007
6	0.084	0.005	0.002	0.000	0.002	0.120	0.024	0.023	0.001	0.007

38

39

40   Table S4 and Table S5 list the linear equations and exponential equation for metal relations in
41 slag samples, based on the figures presented in the paper. As the coefficient of determination is rather
42 low, they are just included as supplementary material and it can not be stated, that neither a linear
43 nor an exponential relation is the right model to express the relations of metal in the slag.

44   **Table S4.** Linear Equations of Metal Relations in Slag Samples and Coefficient of Determination.

Involved Metals	Equation	Coefficient of Determination
Co/Fe	wt.% Co = 0.7319 · wt.% Fe + 0.0109 wt.%	0.8362
Co/Mn	wt.% Co = 0.6543 · wt.% Mn - 0.2006 wt.%	0.3673
Ni/Fe	wt.% Ni = 0.0542 · wt.% Fe + 0.0100 wt.%	0.6162
Ni/Mn	wt.% Ni = 0.0574 · wt.% Mn - 0.0175 wt.%	0.3799

45   **Table S5.** Exponential Equations of Metal Relations in Slag Samples and Coefficient of Determination.

Involved Metals	Equation	Coefficient of Determination
Co/Fe	wt.% Co = $0.1052e^{1.3920 \cdot \text{wt.\% Fe}}$	0.7195
Co/Mn	wt.% Co = $0.0742e^{1.2041 \cdot \text{wt.\% Mn}}$	0.2958
Ni/Fe	wt.% Ni = $0.0114e^{1.1930 \cdot \text{wt.\% Fe}}$	0.4729
Ni/Mn	wt.% Ni = $0.0065e^{1.2322 \cdot \text{wt.\% Mn}}$	0.2772

46
47

48 **2. Supplementary Information about the Metal**

49 This chapter includes the macrographs and micrographs of selected metal samples obtained
50 from the trial and the description of the second melting operation, to obtain the mass of the cobalt-
51 and copper individual phase. A comparison of different analytical methods is presented as well, even
52 though only inductively coupled plasma optical emission spectrometry was used to obtain results in
53 the paper.
54
55 Figure S2 shows a macrograph of the metal obtained from trial number 3, which was solidified
56 in the graphite crucible in the electric arc furnace after the trial.
57

58
59 **Figure S2.** Macrograph of metal obtained from trial number 3.

60 Figure S3 shows a macrograph of the metal obtained from trial number 4. Trial number 4 was
61 tapped after the holding time and the material solidified in a cast-iron-mould. Therefore, the cooling
62 rate of the material was considerably higher compared to the cooling time from trial number 3.
63
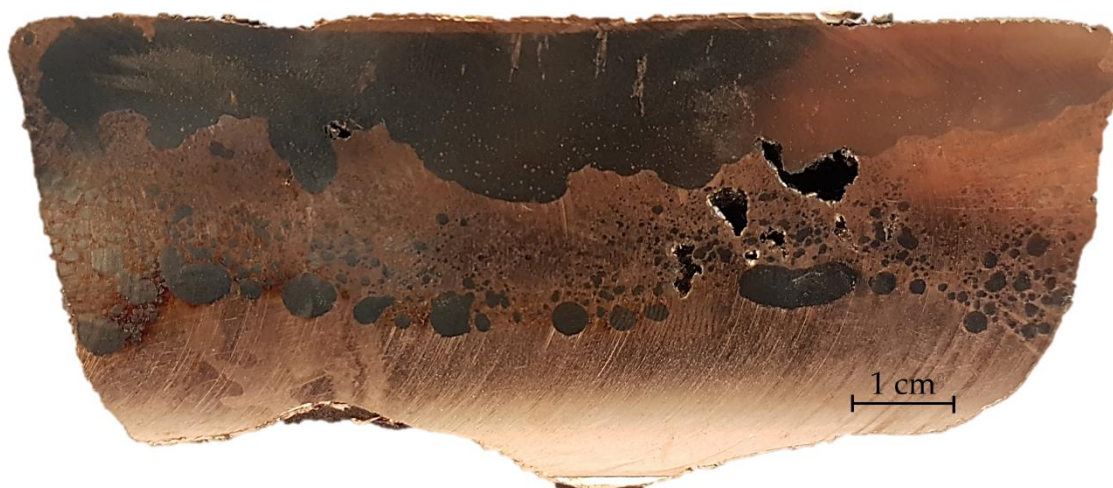
64
65 **Figure S3.** Macrograph of metal obtained from trial number 4.

66   Micrographs of metal samples have been taken with a "VHX-600" digital microscope equipped
67 with a "VH-Z100R" universal zoom lens, both made by "KEYENCE Corporation KK, Osaka,
68 Germany". The metal samples were mechanically sawed in half before they were microscopically
69 investigated. As they were not professionally prepared for optical microscopy, those micrographs are
70 not included in the paper and are just included in the supplementary material. Figure S4 shows a
71 section of the interface between the cobalt- and copper phase of the metal ingot generated in trial
72 number 3. Especially in the copper matrix, a considerable amount of cobalt inclusions is visible,
73 whereas in the cobalt phase only a few copper inclusions are visible.
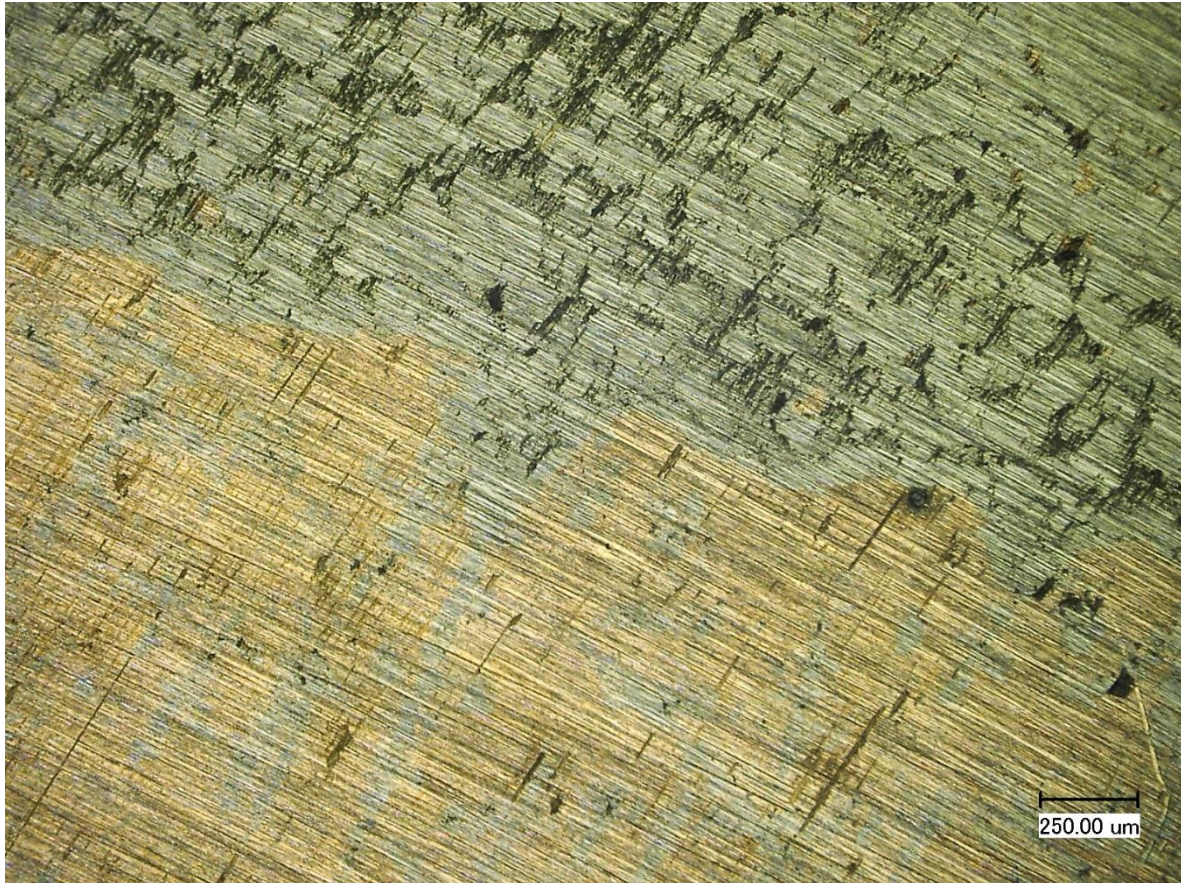

74

75   **Figure S4.** Micrograph of the interface between the cobalt and copper phase of trial number 3.

76

77   Figure S5 and Figure S6 show a section of the cobalt- and copper matrix respectively of the metal
78   ingot generated in trial number 4. In both cases, inclusions are visible in the figures.

79

80   **Figure S5.** Micrograph of the cobalt matrix including copper inclusions of trial number 4.
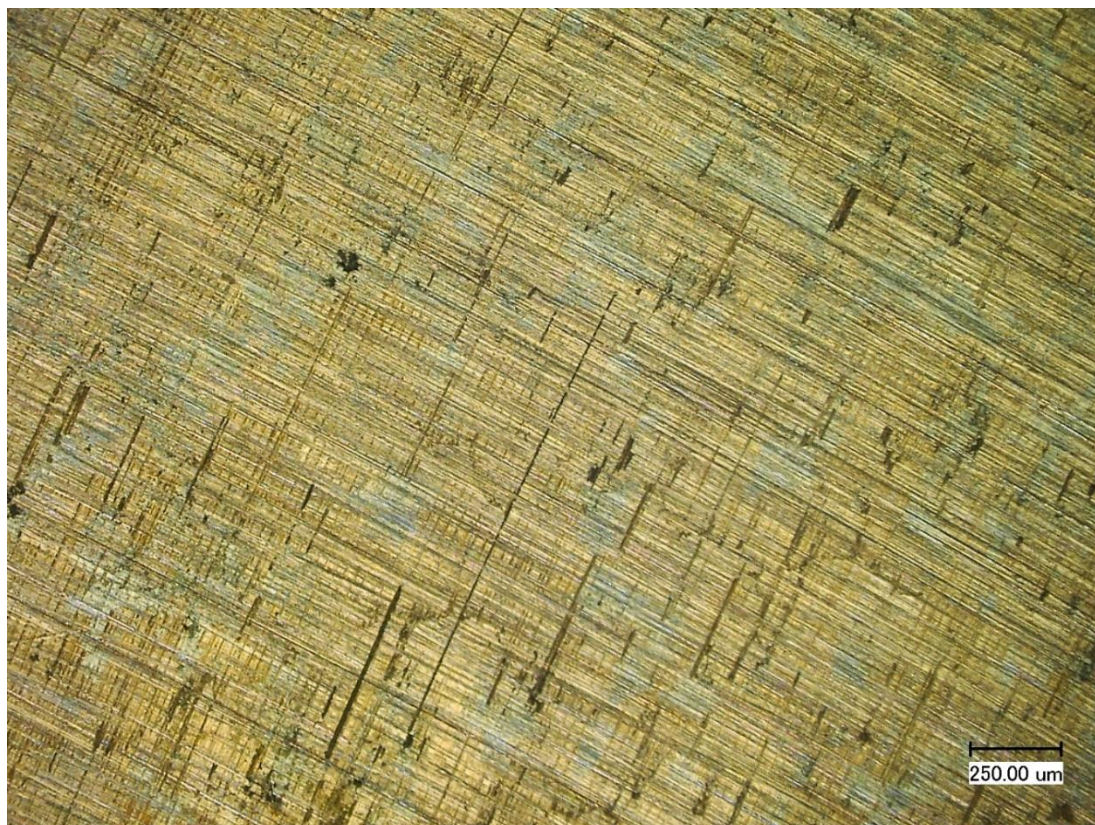
81

82   **Figure S6.** Micrograph of the copper matrix including cobalt inclusion of trial number 4.

Figure S7 shows a section in the bottom area of the metal sample generated in trial number 4. Even at the bottom of the sample cobalt inclusions are visible. Furthermore, solidification voids are present in this section of the sample.

Figure S7. Micrograph of the bottom of the solidified ingot form trial number 3.

89   Figure S8 shows a macrograph of the metal from trial number 3 and trial number 4 after melting
90   in a resistance heated furnace. The furnace type "161-25/20/37-KS" made by "Solo Swiss SA,
91   Porrentruy, Switzerland" was used for the melting procedure. The metal was melted in a graphite
92   crucible and argon was constantly blown into the furnace, to protect the metal from oxidation. The
93   heating rate used was 300 K/h up to the final temperature of 1400 °C, the temperature was then
94   constant for 1 h and afterward, the furnace was cooled with a cooling rate of 300 K/h. The sample was
95   then cut in half to identify the phase boundary. By cutting both blocks at the phase boundary, the
96   cobalt- and copper samples were obtained and weighed. For chemical analysis by ICP-OES, drilling
97   chips of the samples were taken.

99   **Figure S8.** Macrograph of slowly solidified metal from trial 3 and 4.

100   In addition, the metal was also analyzed by X-ray fluorescence (XRF) spectrometry and arc spark
101   optical emission spectrometry (spark-OES). Table S6 shows the metal composition obtained by
102   different analytical methods. The inductively coupled plasma optical emission spectrometry (ICP-
103   OES) analysis was used in the paper. Furthermore, results by a "SPECTROMAXx" spark-OES made
104   by "SPECTRO Analytical Instruments GmbH, Kleve, Germany" are presented. X-ray fluorescence
105   (XRF) results were obtained using the energy dispersive XRF-spectrometer "SPECTRO XEPOS"
106   made by "SPECTRO Analytical Instruments GmbH, Kleve, Germany". XRF and Sparc-OES
107   measurements match the ICP-OES analysis fairly well for the copper sample, except the silicon
108   content, which was significantly lower according to the XRF-measurement. The results of the cobalt
109   sample differ significantly. Especially the measured copper- and silicon content is not accurate in the
110   additional measurements done by XRF and Sparc-OES. Reasons for that could be, that the cobalt alloy
111   calibration for the Sparc-OES does not include copper contents that high. A possible explanation for
112   the lower concentration of silicon measured by XRF in both phases could be the low atomic mass of
113   silicon.

114

Table S6. Comparison of selected elements in metal samples analyzed by different methods.

Element	Cu-Phase			Co-Phase		
	XRF	Spark-OES	ICP-OES	XRF	Spark-OES	ICP-OES
Cu	93.0	92.8	92.44	27.8	1.9	19.90
Co	3.4	2.5	3.22	42.4	44.2	48.87
Ni	1.4	1.3	1.45	4.9	4.6	4.97
Fe	1.1	0.8	1.07	18.8	13.4	19.37
Mn	0.8	0.8	0.69	0.7	0.8	0.35
Si	0.0	1.4	1.35	2.7	33.0	6.17

115

116